ISSN 0021-3640, JETP Letters, 2014, Vol. 100, No. 7, pp. 455–462. © Pleiades Publishing, Inc., 2014.
Original Russian Text © V.V. Val'kov, M.S. Shustin, 2014, published in Pis'ma v Zhurnal Eksperimental'noi i Teoreticheskoi Fiziki, 2014, Vol. 100, No. 7, pp. 510–517.

Radiation-Induced Modification of the Temperature Dependence of the Magnetic Susceptibility of a 1D Magnet

V. V. Val'kov[a, *] and M. S. Shustin[a, b]

[a] *Kirensky Institute of Physics, Siberian Branch, Russian Academy of Sciences, Akademgorodok, Krasnoyarsk, 660036 Russia*

* *e-mail: vvv@iph.krasn.ru*

[b] *Siberian Federal University, Svobodnyi pr. 79/10, Krasnoyarsk, 660041 Russia*

Received February 17, 2014; in final form, September 1, 2014

The excitation spectrum of a catena-$[Fe^{II}(ClO_4)_2\{Fe^{III}(bpca)_2\}]ClO_4$ anisotropic 1D magnet with alternating high-spin and low-spin iron ions has been calculated with the use of the diagrammatic technique for Hubbard operators. This has allowed establishing conformity with the Ising model, for which the magnetic susceptibility has been calculated by the transfer-matrix method. The introduction of a statistical ensemble taking into account the presence of chains with different lengths and iron ions with different spins has allowed describing the modification of the magnetic susceptibility under optical irradiation.

DOI: 10.1134/S0021364014190138

1. INTRODUCTION

Investigation of the elementary excitation spectrum and low-temperature behavior of the magnetic susceptibility of quasi-low-dimensional magnetic structures led to a conclusion of the possibility of existence of coherent spin states in such systems, which do not have analogs in classical magnets [1–6]. Progress in synthesis of organic magnetic compounds [7] made possible experimental investigation of strongly anisotropic single chain magnets (SCMs), the majority of which possess single-ion easy-axis anisotropy. At low temperatures but in the absence of a long-range 3D magnetic order, there appear excited magnetic states in such materials, the lifetime of which can be as long as several hours [8]. Single chain magnets, whose magnetic states can be changed under external irradiation, are of particular interest [9–11]. This explains interest in SCMs not only from the fundamental point of view but also regarding their use as the elemental base of spintronics and memory devices [12].

Specific features of the temperature dependence of the static magnetic susceptibility $\chi(T)$ and relaxation time $\tau(T)$ contain important information on the character of magnetic interactions in SCMs. Such experimental data are most often deciphered on the basis of a 1D Ising model and its kinetic version [6, 13]. It is noteworthy that isolated Ising chains also exist in inorganic compounds [6, 14, 15].

Recent experimental investigation of a catena-$[Fe^{II}(ClO_4)_2\{Fe^{III}(bpca)_2\}]ClO_4$ (hereinafter, SCM-catena) 1D magnet demonstrated a strong change in the magnetic susceptibility $\chi(T)$ under the action of external irradiation [16]. Interpretation of this effect was based on the assumption of a photoinduced change in the magnetic state of the system that occurs as a result of a charge transfer from one metal ion to another (metal-to-metal charge transfer, MMCT) (Fig. 1) [16]. It was assumed that each photon absorbed by the system induces a transition of an electron from the electronic shell of a high-spin (HS) Fe^{II} ($S = 2$) ion to the electronic shell of a low-spin Fe^{III} ($S = 1/2$) ion. In this case, the first iron ion appears in the $S = 5/2$ state and the second one in the $S = 0$ state.

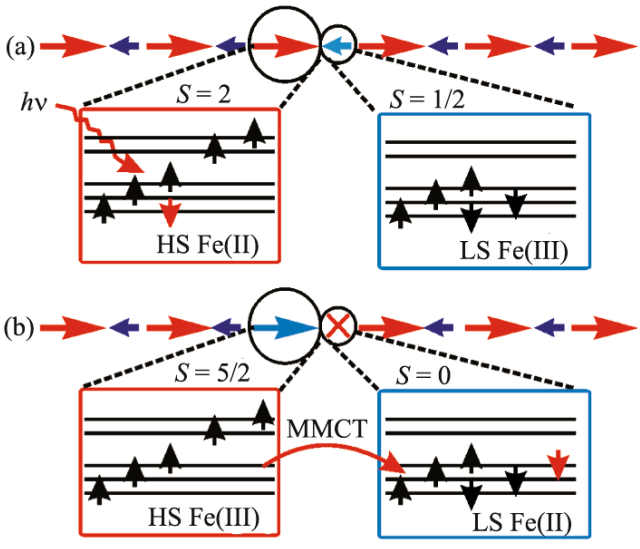

Fig. 1. (Color online) Scheme of a photoinduced metal-to-metal charge transfer (MMCT) process [16].

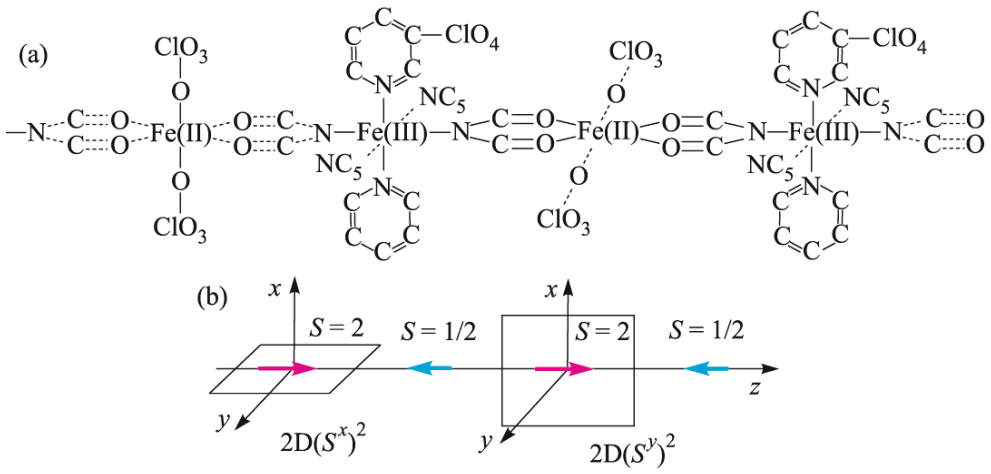

Fig. 2. (Color online) (a) Crystal and (b) magnetic structure of a SCM-catena single-chain magnet [18].

The emergence of iron ions in the nonmagnetic state implies the emergence of broken exchange bonds with the formation of finite chains of various lengths.

In this work, we calculate the spectrum of magnetic excitations of four-sublattice SCM-catena with the use of the diagrammatic technique for Hubbard operators [17], which provides a rigorous description of anisotropic systems with an arbitrary nonequidistance of single-ion energy levels, taking into account different orientations of the easy planes of two neighboring high-spin iron ions. Owing to different orientations of the above easy planes, the excitation spectrum nearly coincides with the excitation spectrum of an easy-axis ferrimagnet, whose effective anisotropy parameter is comparable with the exchange integral. In both cases, a significant gap in the excitation spectrum exceeds the spin-wave bandwidth. This implies that the magnet under consideration appears in the Ising regime. This analogy allows using the transfer-matrix method to calculate exact thermodynamic functions in the entire temperature range. In particular, the inclusion of the specificity of the ligand environment of iron ions in SCM-catena and a radiation-induced change in their charge distribution allowed describing an experimentally observed abnormally high change in the magnetic susceptibility of SCM-catena. The appearance of iron ions in different charge and spin states and finite spin chains of different lengths required introducing a grand canonical ensemble.

2. SPIN HAMILTONIAN OF SCM-CATENA

Magnetically active iron ions in a catena-$[Fe^{II}(ClO_4)_2\{Fe^{III}(bpca)_2\}]ClO_4$ quasi-one-dimensional magnet [18] are alternately in different valence states (Fig. 2). Fe^{II} ions are surrounded by oxygen ions forming a distorted octahedron. The d electrons of such ions experience a weak crystal field and the d^6 configuration corresponds to a high-spin state with $S = 2$. In this case, according to the data of high-frequency ESR spectroscopy, the distortion of the ligand environment of Fe^{II} ions leads to the formation of single-ion easy-plane anisotropy [18].

Fe^{III} ions are surrounded by nitrogen ions with a larger charge as compared to oxygen ions. As a result, the electronic shell of d^5 Fe^{III} ions appears in a strong crystal field. In this case, the ground-state term corresponds to the low-spin state with $S = 1/2$ (Figs. 1 and 2).

Importantly, the easy planes of two neighboring high-spin iron ions are orthogonal (Fig. 2). Such an alternation induces the effective easy axis (see below) oriented along the chain (the z axis in Fig. 2), and there appears a ferromagnetic order at $T < 7$ K [19], as is shown in Fig. 2b.

The second important feature is associated with the fact that the character of the temperature dependence of the relaxation time in the low-temperature region demonstrates slow magnetization dynamics and is described well by the model of a quasi-one-dimensional Ising magnet [18, 19]. As the starting model describing the system of different-valence iron ions in SCM-catena, we choose the Heisenberg model with the uniaxial anisotropy [18, 20]

$$\hat{\mathcal{H}}_{\rm H} = J\sum_{f}[\mathbf{S}_{f,A}\mathbf{S}_{f,B} + \mathbf{S}_{f,B}\mathbf{S}_{f,C} + \mathbf{S}_{f,C}\mathbf{S}_{f,D} + \mathbf{S}_{f,D}\mathbf{S}_{f+1,A}] + 2D\sum_{i}[(S^x_{f,A})^2 + (S^y_{f,C})^2] + \hat{\mathcal{H}}_{\rm Z}. \quad (1)$$

Here, $\mathbf{S}_{f,A}$ and $\mathbf{S}_{f,C}$ are the vector operators of the spin moments of iron ions in the high-spin states with the spin $S = 2$ situated in the positions A and C of the magnetic cell f (the cell includes four magnetic ions), respectively. These ions are subject to the single-ion

easy-plane anisotropy. The intensity of the anisotropy is described by the parameter D. The easy plane of iron ions in the position A (C) is the YOZ (XOZ) plane. In Eq. (1), $\mathbf{S}_{f,B}$ and $\mathbf{S}_{f,D}$ are the vector operators of the spin moments of iron ions in the low-spin states with $S = 1/2$ situated in the positions B and D, respectively. The operator $\hat{\mathcal{H}}_Z$ corresponds to the Zeeman interaction energy. According to the calculations [18–20], $J = 20$ K and $D = 7$ K.

3. LOW-TEMPERATURE SPECTRAL PROPERTIES OF SCM-CATENA

To substantiate the assumption of the formation of an easy axis used in the present study, we calculate the quantum excitation spectrum of model (1). For this purpose, we use the diagrammatic technique for Hubbard operators [17]. As is known, this approach can correctly take into account a strong single-ion anisotropy [21–23] inherent in SCM-catena. Hamiltonian (1) in the representation of Hubbard operators takes the form

$$\hat{\mathcal{H}}_H = \sum_{f,i,n} E_{in} X_{fi}^{nn} + \sum_{f,i,g,j,\alpha,\beta} V_{i\alpha,j\beta}(f,g)\Delta X_{fi}^{\alpha}\Delta X_{gj}^{\beta}. \quad (2)$$

The first term in Eq. (2) corresponds to the single-site part of Hamiltonian (1) with E_{in} being the energy levels of the nth iron ion situated in the ith sublattice. The second term describes intersite correlations owing to the exchange interaction [24]. Here, $\Delta X_{fi}^{\alpha} = X_{fi}^{\alpha} - \langle X_{fi}^{\alpha}\rangle$ and the matrix $V_{i\alpha,j\beta}(f,g)$ with the inclusion of four sublattices has the form

$$V_{i\alpha;j\beta}(f,g) = (\mathbf{c}_i(\alpha), \hat{V}_{fi;gj}\mathbf{c}_j(\beta)), \quad (3)$$

where $\mathbf{c}(\alpha) = \{\gamma_{\|}(\alpha); \gamma_{\perp}(\alpha); \gamma_{\perp}^{*}(-\alpha)\}$, and $\gamma_{\|}(\alpha)$ and $\gamma_{\perp}(\alpha)$ are the parameters of the representation of the spin operators S^z and S^+ in terms of the Hubbard operators. The matrix $\hat{V}_{fi;gj}$ in the general case has the components

$$\hat{V}_{fi;gj} = J_{fi;gj}[1, 0, 0;\quad 0, 1/2, 0;\quad 0, 0, 1/2],$$

where $J_{fi;gj}$ are the exchange integrals for the interaction between the ions of the ith and jth kinds belonging to the fth and gth magnetic cells, respectively. Below, we restrict ourselves to the consideration of the interaction between the nearest neighbors.

To calculate the excitation spectrum, we introduce the Matsubara Green's functions [24]

$$D_{i\alpha;j\beta}(f\tau; g\tau') = -\langle T_{\tau}\hat{X}_f^{\alpha}(\tau)\tilde{X}_g^{-\beta}(\tau')\rangle \quad (4)$$

and write the set of equations for these functions in the zero-loop approximation in the quasimomentum representation. The graphical form of this set is

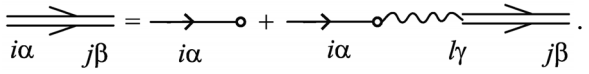

Replacing the graphical elements by the analytical expressions, we find

$$D_{i\alpha;j\beta}(q; i\omega_n) = \delta_{ij}\delta_{\alpha\beta}D_{i\alpha}(i\omega_n)b_{i\alpha} + D_{i\alpha}(i\omega_n)b_{i\alpha}\sum_{l\gamma}V_{i\alpha;l\gamma}(q)D_{l\gamma;j\beta}(q; i\omega_n). \quad (5)$$

Here,

$$D_{i\alpha(n,m)} = [i\omega_n + (E_{in} - E_{im})]^{-1}, \qquad b_{i\alpha(n,m)} = N_{in} - N_{im}, \quad (6)$$

$V_{i\alpha;l\gamma}(q)$ is the Fourier transform of matrix (3), and N_{in} are the occupation numbers of single-site states.

The solution of the set of equations (5) can be greatly simplified by using the form of matrix elements (3) split in the indices of root vectors. Generalizing the method [21, 22] to the case of four sublattices, we find the equation for the excitation spectrum of SCM-catena

$$\det\left\|[\hat{U}, \hat{0}, \hat{0}; \hat{0}, \hat{\Phi}, \hat{W}; \hat{0}, \hat{W}, \hat{\Phi}]\right\| = 0, \quad (7)$$

where

$$\frac{\hat{U}(\omega)}{J} = \begin{pmatrix} -1 & u_A & 0 & u_A e^{-4iq} \\ u_B & -1 & u_B & 0 \\ 0 & u_A & -1 & u_A \\ u_B e^{4iq} & 0 & u_B & -1 \end{pmatrix}, \quad (8)$$

$$\hat{W}(\omega) = \frac{J}{2}\begin{pmatrix} 0 & w & 0 & we^{-4iq} \\ 0 & 0 & 0 & 0 \\ 0 & -w & 0 & -w \\ 0 & 0 & 0 & 0 \end{pmatrix}. \quad (9)$$

The functions involved in the above equations have the form

$$u_{A,B}(\omega) = \sum_{\alpha}\left|\gamma_{\|A,B}(\alpha)\right|^2 D_{A,B}(\alpha)b_{A,B}(\alpha);$$

$$z_{A,B}(\omega) = \sum_{\alpha}\left|\gamma_{\perp A,B}(\alpha)\right|^2 D_{A,B}(\alpha)b_{A,B}(\alpha); \quad (10)$$

$$w(\omega) = \sum_{\alpha}\gamma_{\perp A}(\alpha)\gamma_{\perp A}(-\alpha)D_A(\alpha)b_A(\alpha).$$

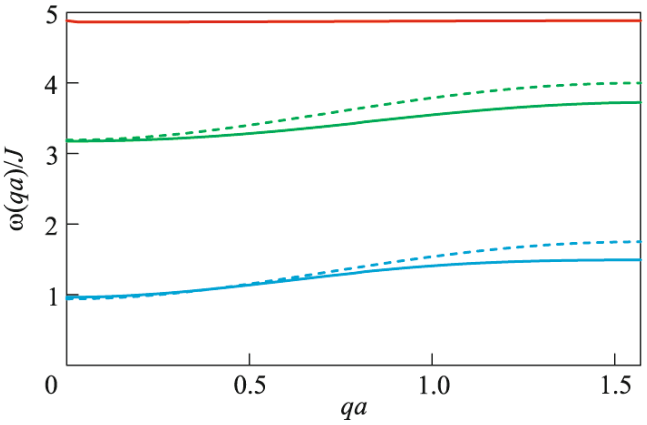

Fig. 3. (Color online) Elementary excitation spectrum of SCM-catena.

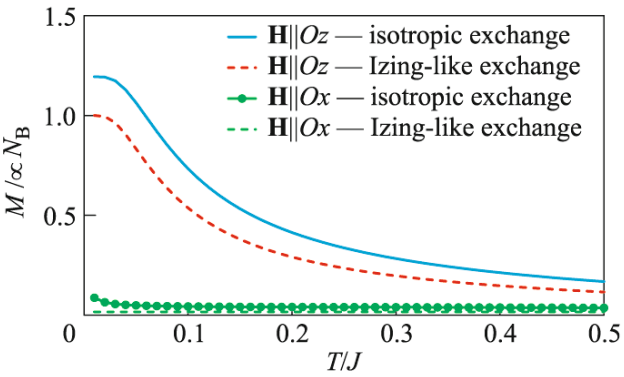

Fig. 4. (Color online) Temperature dependence of the magnetization $M(T)$ of a six-site chain.

The matrix $\hat{\Phi}(\omega)$ can be found from $\hat{U}(\omega)$ by the replacement $J \longrightarrow J/2$ and $u_{A,B}(\omega) \longrightarrow z_{A,B}(\omega)/2$.

The results of the numerical solution of Eq. (7) with $D/J = 1/3$ are shown in Fig. 3. Solid lines represent the quasimomentum dependences of the branches of the excitation spectrum of SCM-catena. Dotted lines are the quasimomentum dependences of the spectrum branches for the effective model of a Heisenberg ferrimagnetic chain with an easy-axis single-ion anisotropy. We set $D \longrightarrow D_{\text{eff}} = -J/8$ and replaced the operator expressions $D(S_k^x)^2$ and $D(S_l^y)^2$ in Eq. (1) by $D_{\text{eff}}(S_k^z)^2$ and $D_{\text{eff}}(S_k^y)^2$, respectively. Comparison of the dependences shown in Fig. 3 indicates that SCM-catena does exhibit the properties typical of an easy-axis ferrimagnet in the low-temperature region.

4. EFFECTIVE MODEL. INTRODUCING A STATISTICAL ENSEMBLE OF ISING CHAINS

The above results indicate that the low-temperature excitation spectrum of SCM-catena corresponds to the spectrum of a 1D-ferrimagnet with the effective easy axis directed along the chain axis. The excitation spectrum of both models is characterized by the presence of the gap Δ and small dispersion of the main excitation branches, as compared to Δ. This implies that, on the qualitative level, the energy structure of a SCM-catena single-chain magnet is reproduced by the single-particle excitation spectrum of a ferrimagnetic Ising chain, for which $\Delta = 2JS_1S_2$ and the dispersion is completely absent.

The validity of this statement can be demonstrated quite well by the analysis of a six-site chain. It turned out that spin fluctuations at the parameter ratio $D/J = 1/3$ are manifested by the fact that the average value of the z spin projection of the high-spin-state ion with $S = 2$ decreases to $\langle S^z \rangle \approx 3/2$ in the ground state of the system. Therefore, below, we assume that the SCM-catena magnet under consideration is described by the spin chain with alternating pseudospins $\tilde{S} = 3/2$ and $\sigma = 1/2$ with the Ising exchange interaction between them.

The direct proof of the possibility of the proposed simplification is associated with the numerical calculation for a finite number of sites. Comparison of the temperature dependences of the magnetization $M(T)$ of the six-site chain is shown in Fig. 4. In the first case, the calculation was performed for Hamiltonian (1). In the second case, we used the generalized Ising model. As is seen, the magnetization curves calculated according to these two approaches agree well with each other for the external magnetic field applied both along and perpendicular to the chain direction.

Under irradiation, an electron is knocked out of the electronic shell of the high-spin state of Fe^{II} and the ion transforms to the valence state Fe^{III} with the spin $S = 5/2$. The released electron is absorbed by an iron ion surrounded by nitrogen complexes, thus inducing its transition to the state Fe^{II} with the spin $S = 0$. We will consider the emergence of ions with new spin configurations in the chain as the emergence of impurities, the density of which depends on the radiation intensity.

Below, we also have to take into account the presence of natural nonmagnetic impurities and defects. Let these inclusions appear at the synthesis of the compound, have a relatively low density ($c \sim 10^{-3}$–10^{-2} per unit length of the chain) [8], and thus be uncorrelated and distributed uniformly in the chains.

We will assume that the probability of a certain number of impurities per unit volume of the sample obeys the Poisson distribution. Since the magnet under consideration is quasi-one-dimensional, this is equivalent to the statement that the nonmagnetic

impurities divide the chain into segments with the number N of sites and the probability P_N of finding the segments with N sites obeys the Poisson statistics $P_N = \overline{N}^N e^{-\overline{N}}/N!$. Here, $\overline{N}$ specifies the average number of particles per chain segment bounded by nonmagnetic impurities.

It is important for the further consideration that the experimental investigation of the optical impact on SCM-catena was performed after prolonged irradiation lasting for several hours. Within this time, photoinduced high-spin (HS Fe^{III}) and low-spin (LS Fe^{II}) states of iron ions appear and recombine repeatedly. Therefore, on average, each iron ion participates in the MMCT processes and, remaining at the same site, changes its state owing to the incoming and outgoing electrons. This situation can be described by introducing a special statistical ensemble. Individual members of this ensemble are spin chains, the sites of which can be occupied by iron ions in each of the above four spin states. Bringing such a system in contact with the thermal bath with the permission of exchanging iron ions allows simulating a change in the relative density of ionic pairs in various spin states [25]. It should be emphasized that, in finding a correct alternation of iron ions in different spin states in the present approach, it proved necessary to introduce effective interactions between these ions. Finally, we take into account that the projection S^z of the spin moment of iron ions in the high-spin state Fe^{III} with the total spin $S = 5/2$ is also reduced to the effective value $\tilde{S} = 2$ owing to quantum fluctuations. As a result, we arrive at the model that is described by the following Hamiltonian in the atomic representation:

$$\hat{\mathcal{H}} = \sum_{f=1}^{N}\left\{\hat{\mathcal{H}}(f,f+1) + \hat{\mathcal{H}}(f+1,f)\right\} + \sum_{f=1}^{N}\left\{\mu_B H\hat{\mathbb{O}}_f + \lambda_1 h_f + \lambda_2 Y_f\right\}, \quad (11)$$

where the two-site operators

$$\hat{\mathcal{H}}(f,f+1) = \hat{\mathcal{H}}_J(f,f+1) + \hat{\mathcal{H}}_V(f,f+1) \quad (12)$$

describe the Ising exchange interaction between magnetically active iron ions:

$$\hat{\mathcal{H}}_J(f,g) = J_1\sum_{mM} mM X_f^{mm} Y_g^{MM} + J_2\sum_{mL} mL X_f^{mm} Z_g^{LL},$$

and the repulsive interaction between the pairs of iron ions that cannot stay nearby according to the physical conditions:

$$\hat{\mathcal{H}}_V(f,g) = V(h_f h_g + X_f X_g + Y_f Y_g + Z_f Z_g + h_f X_g + Y_f Z_g). \quad (13)$$

In these expressions, the operators X_f^{mm} (Y_f^{MM}) are the Hubbard projection operators [17] on the vectors of the Hilbert space corresponding to states of iron ions with the spin $S = 1/2$ ($\tilde{S} = 3/2$) and the spin (pseudospin) projection m (M) on the quantization axis. The projection operator Z_f^{LL} corresponds to the state of an iron ion at the site f with $\tilde{S} = 2$ and the pseudospin projection L on the quantization axis. As was mentioned above, this state appears as a result of optical irradiation. The operator h_f is the Hubbard projection operator on the vector $|f, 0\rangle$ of the Hilbert space corresponding to the presence of an iron ion at the site f in the state with the spin $S = 0$. In this case, the operators

$$X_f = \sum_m X_f^{mm}, \quad Y_f = \sum_M Y_f^{MM}, \quad Z_f = \sum_L Z_f^{LL}$$

are projectors on the subspaces with a fixed spin or pseudospin without specifying its projection.

The first term of single-site operators reflects the Zeeman contribution. In the above notation,

$$\hat{\mathbb{O}}_f = g_1\sum_m mX_f^{mm} + g_2\sum_M MY_f^{MM} + g_3\sum_L LZ_f^{LL},$$

where g_1, g_2, and g_3 are the g factors of three magnetic states of an iron ion.

The necessity of the last two single-site operators is associated with the fact that the system is in contact with the thermal bath. Therein, λ_1 and λ_2 are the Lagrange coefficients. They are found from the solution of the set of two equations

$$\langle X_f\rangle = \langle Y_f\rangle, \quad \langle h_f\rangle = \langle Z_f\rangle. \quad (14)$$

These equations control the number of iron ions in various states under the action of radiation. In fact, the appearance of Eq. (14) is associated with the abovementioned (see Fig. 2) features of the MMCT processes.

It is noteworthy that the use of the two-site operator $\hat{\mathcal{H}}_V$ and the operators describing the contact with the thermal bath allows reproducing the sequence of spin states of iron ions that corresponds to the magnetic structure of SCM-catena. The two-site operators $\hat{\mathcal{H}}_V$ take into account correlations in the mutual positions of iron ions of different types (see Figs. 1 and 2)

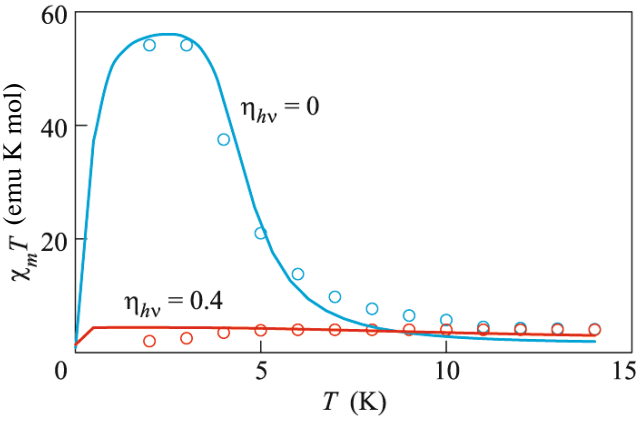

Fig. 5. (Color online) Temperature dependence of the magnetic susceptibility (red) with and (blue) without irradiation according to (solid lines) theory and (circles) experiment. The experimental data were borrowed from [16].

and the parameter V of such an interaction is chosen infinitely high in the final calculations.

The partition function for the introduced ensemble of chains was calculated with the use of the transfer-matrix method [26–28]. This approach provides a simple computation of both averages

$$\left\langle A_f^{(\nu)} \right\rangle_N = \frac{1}{\Xi} \sum_{\alpha=1}^{12} \langle u_\alpha | A^{(\nu)} | u_\alpha \rangle \lambda_\alpha^N \qquad (15)$$

and correlation functions

$$\left\langle A_f^{(\nu_1)} A_{f+d}^{(\nu_2)} \right\rangle_N = \frac{1}{\Xi} \sum_{\alpha,\beta=1}^{12} A_{\alpha\beta}^{(\nu_1)} A_{\beta\alpha}^{(\nu_2)} \lambda_\alpha^{N-d} \lambda_\beta^d,$$

$$\left\langle A_f^{(\nu_1)} A_{f+1}^{(\nu_2)} \ldots A_{f+k-1}^{(\nu_k)} \right\rangle_N \qquad (16)$$

$$= \frac{1}{\Xi} \sum_{\alpha_1 \ldots \alpha_k = 1}^{12} A_{\alpha_1\alpha_2}^{(\nu_1)} A_{\alpha_2\alpha_3}^{(\nu_2)} \ldots A_{\alpha_k\alpha_1}^{(\nu_k)} \lambda_{\alpha_1}^{N-k} \lambda_{\alpha_2} \ldots \lambda_{\alpha_k},$$

built on the operators $A_f^{(\nu)}$, which are diagonal in the space of single-site states of the chain. Here, the ν index enumerates the type of single-site operator $A_f^{(\nu)}$ and $|u_\alpha\rangle$ and λ_α are the eigenvectors and eigenvalues of the transfer matrix, respectively. In the chosen basis of the eigenvectors, $A_{\alpha,\beta}^{(\nu)} = \langle u_\alpha | A^{(\nu)} | u_\beta \rangle$.

In the analysis of the effect of irradiation on the magnetic properties, the density $n_{h\nu}$ of photons inducing the MMCT processes was thought to be identical to the averages, $n_{h\nu} = \langle h_f \rangle = \langle Z_f \rangle$. Accordingly, the averages were calculated from Eq. (15) with the simultaneous solution of system (14) for each given radiation intensity.

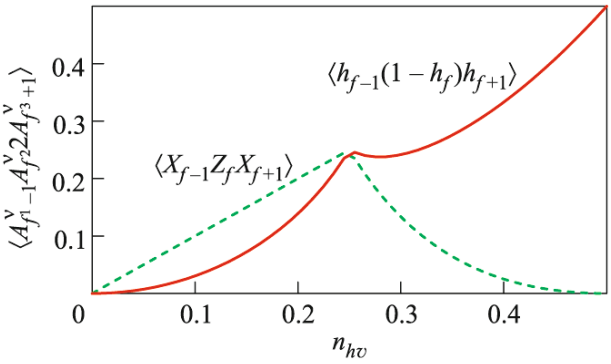

Fig. 6. (Color online) Three-center correlation functions of the systems versus $n_{h\nu}$.

5. RESULTS AND DISCUSSION

The modification of the molar susceptibility $\chi_m(T)$ under irradiation of SCM-catena is shown in Fig. 5. The temperature dependence $\chi_m(T)$ at the given density $n_{h\nu}$ was calculated according to the formula

$$\chi_m(T) = N_A \mu_B \frac{\partial}{\partial H} \sum_N \frac{\bar{N}^N e^{-\bar{N}}}{N!} \langle \mathbb{O}_f \rangle_N \qquad (17)$$

with the use of Eqs. (15) and (14). Variation of the radiation intensity was modeled by changing $n_{h\nu}$. In this approach, $n_{h\nu} = 0$ in the absence of radiation. The best agreement of the theoretical calculations of the modification of $\chi_m(T)$ under irradiation with the experimental results (Fig. 5) was achieved with the following parameters of the model:

$$J_1 = 15 \text{ K}; \quad J_2 = 30 \text{ K}; \quad \bar{N} = 78; \quad H = 100 \text{ Oe};$$
$$g_1 = 3.1; \quad g_2 = 2.9; \quad g_3 = 2.5. \qquad (18)$$

These values agree well with the known experimental data on the system [20, 16]

$$J \approx 20 \text{ K}; \quad g_{1,2,3} \approx 2; \quad \bar{N} \sim 100; \quad H \simeq 100 \text{ Oe}. \qquad (19)$$

One of the reasons for $\chi_m(T)$ weakening under irradiation is the emergence of paramagnetic centers in the chains. The solid line in Fig. 6 shows the radiation-intensity dependence of the probability of appearance of such complexes found by calculating the correlation function $\langle h_{f-1}(1-h_f)h_{f+1} \rangle$ with the use of Eqs. (14) and (16) and subsequent averaging over the Poisson distribution. The analysis of the character of the susceptibility modification under a change in $n_{h\nu}$ showed that the strongest modification of the dependence $\chi(T)$ occurs in the intensity region ($n_{h\nu} < 0.3$), where the probability of appearance of paramagnetic centers increases most quickly. Thus, it should be concluded that, in the present model, the effects of photoinduced formation of paramagnetic complexes play an important role in the modification of the temperature

dependence of the magnetic susceptibility of SCM-catena under irradiation. The dotted line in Fig. 7 shows the dependence of the correlation function $\langle X_{f-1}Z_fX_{f+1}\rangle$ on $n_{h\nu}$. It is noteworthy that the behavior of $\langle Y_{f-1}h_fY_{f+1}\rangle$ is similar to that of $\langle X_{f-1}Z_fX_{f+1}\rangle$ and, for this reason, is not shown. These quantities determine the probability of the formation of complexes when two iron ions in photoinduced spin states are not situated in the neighboring sites. As is seen in the shown dependence, such states also contribute to the low-temperature susceptibility.

6. CONCLUSIONS

In this work, the excitation spectrum of an anisotropic four-sublattice ferrimagnet, the unit cell of which contains two high-spin and two low-spin iron ions, has been calculated with the use of the diagrammatic technique for Hubbard operators. The orientations of the easy planes of high-spin ions are orthogonal to each other. According to the microscopic calculation of the spectrum of this system, the characteristics of the spectrum are similar to the spectrum of an easy-axis magnet with the effective anisotropy on the order of the exchange parameter. Moreover, it turned out that the properties of the magnet with the parameters of the system known from the experiment are close to those described by the generalized Ising model. The validity of this analogy has also been demonstrated by comparing the results of exact numerical calculations of the temperature dependence of the magnetization for the initial anisotropic Heisenberg model and for the generalized Ising model.

This has allowed us to perform calculations in the generalized Ising model with the use of the transfer-matrix method for the investigation of the thermodynamic properties in a wide temperature range. Generalization of this approach to the case where defects appear in the system both at the growth stage and during irradiation allowed describing the experimentally observed variation of the magnetic susceptibility. Therein, to describe the ensemble of chains of different lengths, we have used the Poisson distribution and have taken into account the possibility of redistribution of electrons among the ions in the chains that occurs as a result of photoinduced processes under irradiation. To take into account the specificity of the magnetic structure and radiation-induced changes in the spin states of iron ions, we have introduced nonmagnetic intersite Coulomb repulsive interactions. For convenience of calculations, we have implemented atomic representation, which provides a correct description of multilevel single-ion systems with a nonequidistant energy spectrum.

In conclusion, it is worth mentioning that the approach used in this work is not restricted to the compound under consideration. It can also be applied to the description of the experimentally observed radiation-induced modification of the temperature dependence of the magnetic susceptibility of other single-chain magnets [9–11].

This work was supported by the Russian Foundation for Basic Research, project nos. 12-02-31130, 13-02-00523, and 13-02-98013.

REFERENCES

1. A. I. Smirnov, *Disorder and Order in Quantum Spin Chains* (Mosk. Fiz. Tekh. Inst., Moscow 2004) [in Russian].
2. S.-L. Drechsler, O. Volkova, A. N. Vasiliev, N. Tristan, J. Richter, M. Schmitt, H. Rosner, J. Malek, R. Klingeler, A. A. Zvyagin, and B. Buechner, Phys. Rev. Lett. **98**, 077202 (2007).
3. L. E. Svistov, L. A. Prozorova, A. M. Farutin, A. A. Gippius, K. S. Okhotnikov, A. A. Bush, K. E. Kamentsev, and E. A. Tishchenko, J. Exp. Theor. Phys. **108**, 1000 (2009).
4. A. A. Bush, V. N. Glazkov, M. Hagiwara, T. Kashiwagi, S. Kimura, K. Omura, L. A. Prozorova, L. E. Svistov, A. M. Vasiliev, and A. Zheludev, Phys. Rev. B **85**, 054421 (2012).
5. A. A. Bush, N. Buttgen, A. A. Gippius, V. N. Glazkov, W. Kraetschmer, L. A. Prozorova, L. E. Svistov, A. M. Vasiliev, A. Zheludev, and A. M. Farutin, Phys. Rev. B **88**, 104411 (2013).
6. Yu. B. Kudasov, A. S. Korshunov, V. N. Pavlov, and D. A. Maslov, Phys. Usp. **55**, 1169 (2012).
7. L. Bogani, A. Vindigni, R. Sessoli, and D. Gatteschi, J. Mater. Chem. **18**, 2472 (2008).
8. C. Coulon, H. Miyasaka, and R. Clérac, Struct. Bonding **122**, 163 (2006).
9. T. Liu, Y.-J. Zhang, S. Kanegawa, and O. Sato, J. Am. Chem. Soc. **132**, 8250 (2010).
10. N. Hoshino, F. Iijima, G. Newton, N. Yoshida, T. S. Hiroyuki Nojiri, A. Nakao, R. Kumai, Y. Murakami, and H. Oshio, Nature Chem. **4**, 921 (2012).
11. T. Liu, H. Zheng, S. Kang, Y. Shiota, S. Hayami, M. Mito, O. Sato, K. Yoshizawa, S. Kanegawa, and C. Duan, Nature Commun. **4**, 2826 (2013).
12. W.-X. Zhang, R. Ishikawa, B. Breedlove, and M. Yamashita, RSC Adv. **3**, 3772 (2013).
13. R. Glauber, J. Math. Phys. **4**, 294 (1963).
14. Yu. B. Kudasov, J. Exp. Theor. Phys. **110**, 360 (2010).
15. Yu. B. Kudasov, A. S. Korshunov, V. N. Pavlov, and D. A. Maslov, Phys. Rev. B **83**, 092404 (2011).
16. M. Yamashita, T. Kajiwara, Yu. Kaneko, M. Nakano, Sh. Takaishi, T. Ito, H. Nojiri, N. Kojima, and M. Mito, Presentation at *6th International Symposium on Crystalline Organic Metals, Superconductors, and Ferromagnets, 2005.*
17. R. O. Zaitsev, *Diagram Methods in Theory of Superconductivity and Ferromagnetizm* (Editorial URSS, Moscow, 2004) [in Russian].

18. T. Kajiwara, M. Nakano, Yu. Kaneko, Sh. Takaishi, T. Ito, M. Yamashita, A. Igashira-Kamiyama, H. Nojiri, Yu. Ono, and N. Kojima, J. Am. Chem. Soc. **127**, 10150 (2005).

19. T. Kajiwara, H. Tanaka, and M. Yamashita, Pure Appl. Chem. **80**, 2297 (2008).

20. T. Kajiwara, H. Tanaka, M. Nakano, Sh. Takaishi, Ya. Nakazawa, and M. Yamashita, Inorg. Chem. **49**, 8358 (2010).

21. V. V. Val'kov and T. A. Val'kova, Sov. J. Low Temp. Phys. **11**, 524 (1985).

22. V. V. Val'kov, T. A. Val'kova, and S. G. Ovchinnikov, Sov. Phys. JETP **61**, 323 (1985).

23. V. V. Val'kov and T. A. Val'kova, Sov. J. Theor. Math. Phys. **76**, 766 (1988).

24. R. O. Zaitsev, Sov. Phys. JETP **43**, 574 (1976).

25. A. K. Arzhnikov and A. V. Vedyaev, Sov. J. Low Temp. Phys. **8**, 600 (1982).

26. R. J. Baxter, *Exactly Solved Models in Statistical Mechanics* (Academic, New York, 1982; Mir, Moscow, 1985).

27. F. A. Kassan-Ogly, Phase Trans. **72**, 223 (2000).

28. K. Bernot, J. Luzon, A. Caneschi, D. Gatteschi, R. Sessoli, L. Bogani, A. Vindigni, A. Rettori, and M. G. Pini, Phys. Rev. B **79**, 134419 (2009).

Translated by A. Safonov